X-ray diffraction studies of iodine-doped polyacetylene

P. Robin
Laboratoire Central de Recherche, Thomson-CSF, Domaine de Corbeville-B.P.10, 91401 *Orsay Cedex, France*

J. P. Pouget and R. Comes
Laboratoire de Physique des Solides And Lure, Université Paris Sud, 91405 *Orsay Cedex, France*

and H. W. Gibson and A. J. Epstein
Xerox Webster Research Center, 800 *Phillips Road-W*114, *Webster, NY* 14580, *USA*
(Received 30 November 1982; revised 26 May 1983)

The results of an extensive X-ray and synchrotron radiation diffraction study of the structure of *cis*- and *trans*-polyacetylene doped with iodine are presented. Studies of rapidly and slowly iodine-doped samples confirmed that undoped regions of $(CH)_x$ remain. The undoped regions of the initially *cis*-$(CH)_x$ are shown to isomerize to the *trans*-$(CH)_x$ structure during the doping process. Two new previously unreported X-ray reflections have been recorded for both doped *cis*- and doped *trans*-isomers. The data are in agreement with the model of intercalation of iodine between planes of close-packed polyacetylene chains.

Keywords Polyacetylene; X-ray; iodine-doped; isomerization; structure intercalation

INTRODUCTION

Special interest has been paid to polyacetylene, $(CH)_x$, since the report[1] that its electrical conductivity is increased by more than eight orders to magnitude when doped with iodine or arsenic pentafluoride[2]. $(CH)_x$ may be synthetized[3] as the *cis*-isomer or as the thermodynamically more stable *trans*-isomer, *Figure 1*. Though the detailed crystal structure[3,5-19] of these isomers is not yet resolved, it has been shown[20] that the *cis* structure evolves continuously to the *trans* structure during the isomerization process.

Considerable uncertainty is associated with doped samples. Nuclear magnetic resonance[21], Raman, infrared[23], and optical[24] spectroscopies show a *cis* to *trans* isomerization of the *cis*-polyacetylene chain upon doping, which is not clearly confirmed by structural studies[13]. Reliable comparisons between different studies are difficult because the distribution of the dopant inside a given film may depend on its preparation and on doping conditions[25].

Here the results of an X-ray diffraction study of iodine-doped *cis*- and *trans*-polyacetylene films are presented. Similar samples have been characterized earlier by other studies including fibrillar morphology and the fibril swelling upon doping[26], electrical field dependent conductivity[27], frequency dependent conductivity[28], magnetic susceptibility[25], infra-red absorption[29] and X-ray structure of undoped $(CH)_x$[20]. The results of the X-ray studies of slow- and fast-doped *cis*- and *trans*-$(CH)_x$ show that even at the highest doping level studied $(CHI_{0.2})_x$, undoped regions of $(CH)_x$ remain. The undoped regions of the initially *cis*-$(CH)_x$ are shown to isomerize to the *trans*-$(CH)_x$ structure during the doping process. Two new broad previously unreported X-ray lines associated with iodine doped $(CH)_x$ are reported for both doped *cis*- and doped *trans*-isomers.

These results are shown to be consistent with the model of intercalation of iodine between planes of close-packed $(CH)_x$ chains on a lateral coherence length of about 2.0 ± 0.5 nm. Extensive temperature dependent conductivity, thermopower, and magnetic susceptibility (χ) and room temperature infra-red reflectivity were carried out on samples of the same slowly-doped $(CH)_x$ films reported here. These results[30,31] showed that these nearly metallic

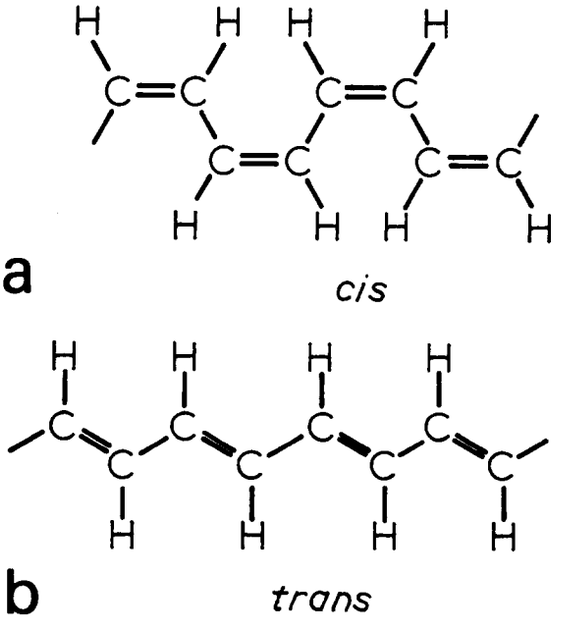

Figure 1 Idealized structure for (a) *cis*-polyacetylene, and (b) *trans*-polyacetylene isomers

0032-3861/83/121558-07$03.00

samples of iodine-doped polyacetylene had high conductivity ($\approx 10\,\text{Ohm}^{-1}\,\text{cm}^{-1}$) and low magnetic susceptibility ($\chi \approx 0.1\chi^{\text{Pauli}}$). Together with the X-ray data presented here, these results support a model[30,31] of charge transport via variable range hopping[32] among pinned charged soliton-like states[33,34] at the Fermi level of these nearly metallic samples.

EXPERIMENTAL

The polyacetylene films were prepared by the method of Shirakawa[14] from acetylene freshly purified by multiple sublimations. The 60–80 μm thick samples were stored at −80°C under argon and handled in an oxygen-free ($\leqslant$0.8 ppm) and water-free ($\leqslant$0.5 ppm) glove box. Scanning electron microscopic (SEM) studies[26] showed that the films were composed of $\approx$40–50 nm diameter, randomly-oriented fibrils. Earlier diffraction studies of oriented fibrils[11] and stretch oriented films[16] show that the polymer chains are parallel to the fibril axis. Isomerization was carried out *in vacuo* in sealed glass ampules at 207°C (refluxing tetralin vapours) for 98 min. The *cis* samples were $\approx$90% *cis*, while the isomerized samples were $\approx$95% *trans*.

The 'slow doping' technique[25] was carried out *in vacuo* by exposure of the film of *cis*- or *trans*-polyacetylene to iodine vapours at 0.1 Torr by maintaining the desired amount of iodine at 13°C (CO_2/xylene) for 15 h, then pumping cryogenically using liquid N_2 on the iodine source for 9 h, exposure to 0.1 Torr of iodine again for 87 h, cryogenic pumping for 6 h and finally dynamic pumping at 10^{-1} Torr for 10 min. The iodine content was determined by weight uptake and confirmed by elemental analysis.

The 'normal' or rapid-doping procedure of *cis*-polyacetylene consisted of flowing iodine vapour from a source at 25°C on a stream of purified argon through a flask containing a reference sample mounted two-probe on platinum wires with Electrodag R conductive paint and the requisite number of additional samples. When the reference sample attained the desired resistivity, the iodine source was shut off and samples were removed under argon flow and placed in glass ampules and flushed with argon for 10 min. These samples were then subjected to dynamic vacuum for 3 min ($\approx 7 \times 10^{-2}$ Pa) and sealed into the ampules. Composition was determined by weight uptake and confirmed by elemental analysis.

X-rays data were collected on photographic film fixed on a cylindrical camera with the sample placed at the centre of the chamber and maintained under vacuum. X-ray patterns were taken using MoKα (0.0707 nm) and CuKα (0.1542 nm) radiations produced either by conventional or rotating anode X-ray sources. To have limited exposure time at ambient temperature together with enough intensity to detect weak reflections, an intense monochromatic X-ray beam was used after (002) reflection on a doubly-bent, graphite monochromator. Additional data were also obtained with the higher resolution X-ray synchroton radiation ($\lambda = 0.1315$ nm) at the station D16 of LURE (ORSAY). X-ray films were read in the equatorial plane of the experimental apparatus, using a Joyce Loeble microdensitometer.

Analysis of X-ray data

Figures 2 and *3* present X-ray patterns from undoped and iodine-doped *cis*-$(CH)_x$ and *trans*-$(CH)_x$ samples obtained with MoKα radiation. As reported by various authors[3,5,19], these X-ray patterns are composed of Debye–Scherrer ring reflections according to the random orientation of polyacetylene fibrils with respect to X-ray beam. Two major results were obtained from these rings:

(a) The diameter of the ring was converted into Bragg angle θ_0. Using the Bragg relation, $\lambda = 2d \sin\theta_0$, where λ is the wavelength of the incident radiation and d is the spacing between diffracting planes, this latter quantity was established. *Tables 1* and *2* report such distances for various samples investigated with CuKα and synchrotron radiations.

(b) The angular width at half height of the ring, $\Delta(2\theta)$, was always found larger than the experimental resolution $\Delta_R(2\theta)$ which was measured at approximately the same Bragg angle on Debye–Scherrer patterns obtained with Al powder. As usual[35], the intrinsic broadening $\Delta_I(2\theta)$, due to the finite size, L, of the crystalline areas which contribute to Bragg reflections, was obtained after a Gaussian correction:

$$\Delta_I(2\theta) = (\Delta^2(2\theta) - \Delta_R^2(2\theta))^{\frac{1}{2}}$$

The coherence length, L, was deduced from the Scherrer formula: $L = 0.9/\cos\theta_0 . \Delta_I(2\theta)$. As shown by the data in *Tables 1* and *2*, only relatively sharp lines are observed in undoped samples while iodine-rich samples exhibit both sharp and broad lines.

X-ray patterns of undoped samples also had a weak broad ring at $d \approx 0.39$ nm which has been attributed to X-ray diffraction of amorphous regions in the sample[17]. This amorphous ring appears as a weak shoulder on the left side of the strongest reflection of *cis*-$(CH)_x$ and *trans*-$(CH)_x$ shown in *Figures 4a* and *5a*, respectively. The amount of crystallinity was then estimated by comparing the integrated intensity of this diffuse halo with the integrated intensity of Debye–Scherrer rings. However, an accurate determination of this ratio needs a detailed analysis of the X-ray pattern and a hypothesis concerning the shape of chains[20], which have not been carried out.

RESULTS

Cis-$(CH)_x$ *samples*

Figure 2a shows the well-defined Debye–Scherrer X-ray pattern from a 90% *cis*-rich $(CH)_x$ which resembles in intensity and position those reported for *cis* samples by Baughman *et al.*[5] and Haberkorn *et al.*[17]. Spacings of the undoped *cis*-$(CH)_x$ calculated from patterns obtained with CuKα radiation, *Table 1*, are in good agreement with those found by Baughman *et al.*[5] and Lieser *et al.*[9]. However, in this study the (001) reflection (c-axis is taken along chain direction) reported by Lieser *et al.*[9] was not detected in any of the samples.

According to the indexation carried out by Baughman *et al.*[5] and Lieser *et al.*[9], most of reflections observed have no index in the chain direction. Thus, they correspond to spacing perpendicular to chain direction. As a consequence, the Scherrer formula applied to their width gives transverse coherence lengths, i.e. perpendicular to the fibril axis. In the present case, the width of the strongest reflections gives the same transverse coherence length of $\approx 8.0 \pm 0.1$ nm, in good agreement with that found by Haberkorn *et al.*[17]. This value is approximately

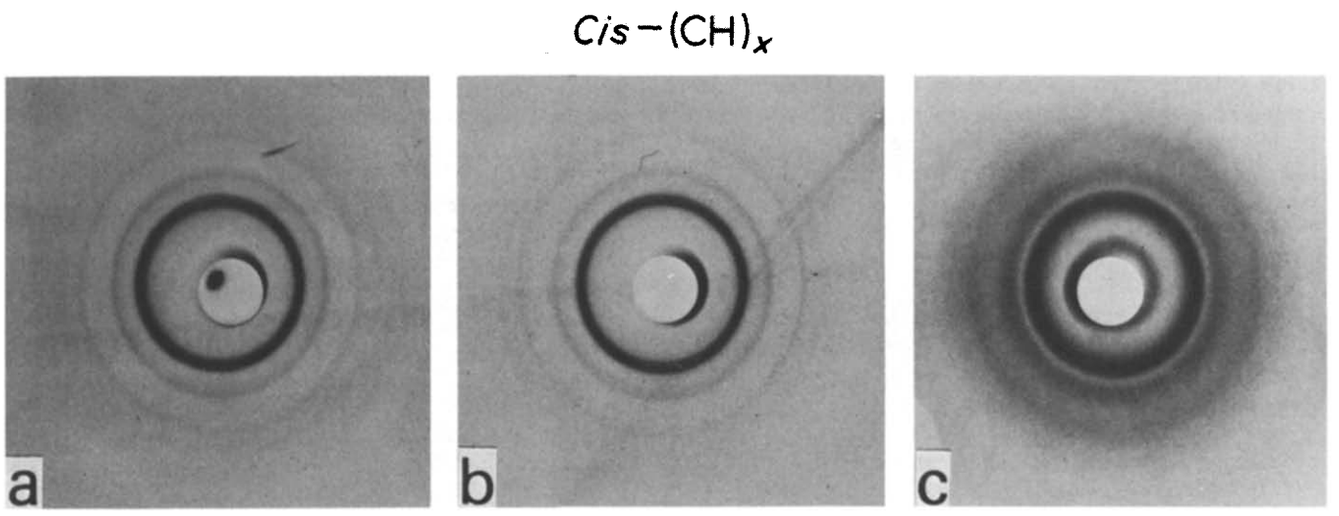

Figure 2 Debye–Scherrer patterns obtained with MoKα radiation for 90% *cis*/10% *trans*-$(CH)_x$. (a) Undoped; (b) rapidly doped with iodine in 86 min to $(CHI_{0.010})_x$ and a resistivity of 2.9×10^2 ohm-cm; (c) rapidly doped with iodine in 22 h, 51 min to $(CHI_{0.194})_x$ and a resistivity of 6.3×10^{-2} ohm-cm

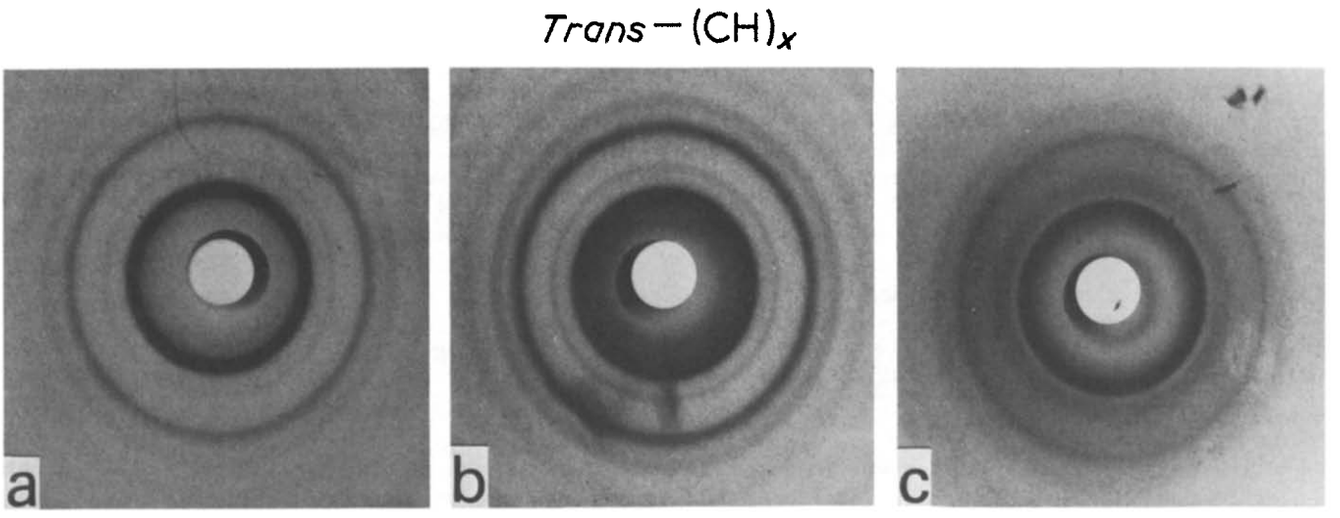

Figure 3 Debye–Scherrer patterns obtained with MoKα radiation for (a) *trans*-$(CH)_x$ undoped; (b) rapidly iodine-doped *trans*-$(CH)_x$, to a composition of $(CHI_{0.009})_x$ and resistivity of 80 ohm-cm; and (c) *trans*-$(CH)_x$ rapidly doped to a composition of $(CHI_{0.050})_x$ and a resistivity of 0.7 ohm-cm

Table 1 Spacing between Bragg reflection planes in nm and intensity (S, strong; M, medium; W, weak; VW, very weak) deduced from position in reciprocal space of Debye–Scherrer rings of 90% *cis*–$(CH)_x$ and slowly-doped 90% *cis*–$(CHI_{0.099})_x$ and 90% *cis*–$(CHI_{0.143})_x$. The symbol ~ in front of 3 distances of doped–$(CH)_x$, means that corresponding rings are broad

Cis–$(CH)_x$ *d* (nm)	*Cis*–$(CH_{0.099})_x$ *d* (nm)	*Cis*–$(CH_{0.143})_x$ *d* (nm)
	~0.79 M	~0.785 M
	~0.41 M	~0.41 M
0.381 S	0.365 S	0.368 S
0.312 W		
0.287M	~0.29 M	~0.29 M
0.244 VW	0.223 VW	
0.220 M	0.213 W	0.212 W
0.213 VW	0.183 W	0.182 W
0.200 VW	0.149 VW	
0.190 W	0.132 VW	
0.174 W		
0.165 W		
0.150 VW		
0.136 W		
0.122 W		

Table 2 Spacing between Bragg reflection planes in nm, and intensity (S, strong; M, medium; W, weak; VW, very weak) deduced from position in the reciprocal space of Debye–Scherrer rings of *trans*–$(CH)_x$, slowly-doped *trans*–$(CHI_{0.050})_x$ and slowly-doped *trans*–$(CHI_{0.125})$. The symbol ~ in front of 3 distances of doped–$(CH)_x$, means that corresponding rings are broad

Trans–$(CH)_x$ *d* (nm)	*Trans*–$(CHI_{0.050})_x$ *d* (nm)	*Trans*–$(CHI_{0.125})_x$ *d* (nm)
	~0.79 M	~0.78 M
	~0.41 M	~0.41 M
0.372 S	0.377 S	0.373 S
0.356 S	0.359 S	0.356 S
	~0.29 M	~0.29 M
0.274 W	0.278 W	
0.212 M	0.213 W	0.212 W
0.204 W	0.205 VW	
0.187 W	0.188 W	0.184 W
0.179 W	0.180 W	
0.160 W		
0.156 W		
0.138 W		
0.131 W		
0.123 W		
0.119 W		

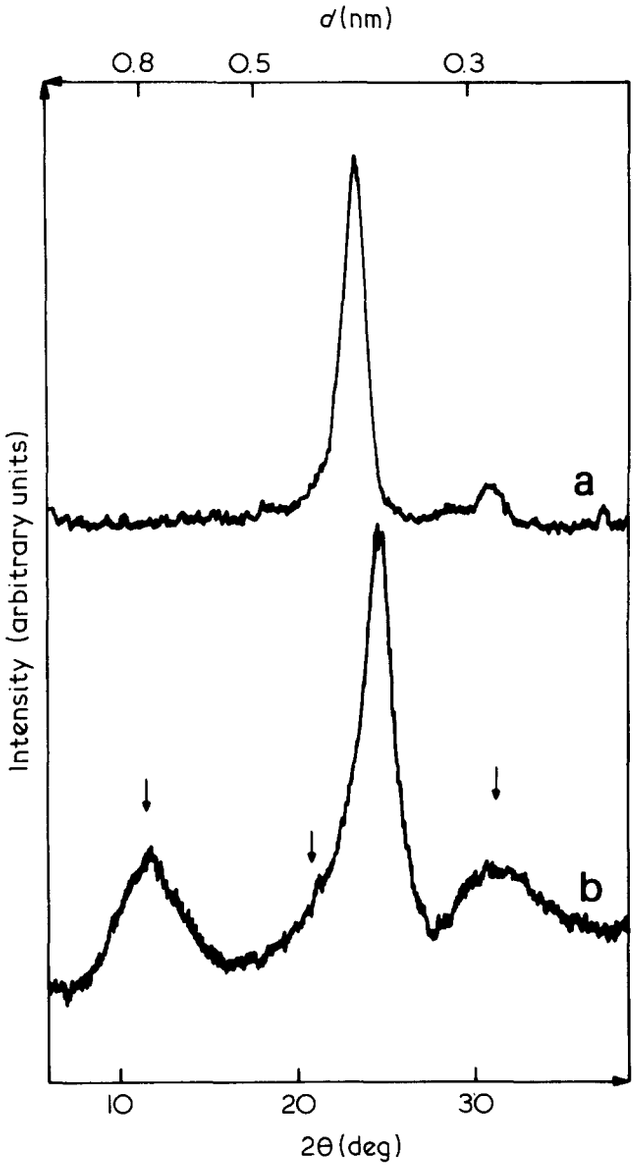

Figure 4 Microdensitometer readings from X-ray patterns of (a) *cis*-$(CH)_x$ and (b) *cis*-$(CH)_x$ slowly doped to $(CHI_{0.099})_x$. Three additional broad reflections are shown by arrows. (λ=0.1542 nm)

one fifth the average diameter of a fibril. The ratio of the integrated intensity of Debye–Scherrer rings to the total intensity gives an X-ray crystallinity of the sample of $\approx$90%.

Iodine-shaped cis-$(CH)_x$ *samples*

At low levels of iodine doping, there is no major modification of the Debye–Scherrer X-ray pattern, *Figure 2b*. At higher levels of iodine doping (samples with greater than approximately ten per cent iodine concentration) the reflections significantly decrease in intensity such that the weak reflections of undoped samples occurring at a large Bragg angle cannot be observed. *Figure 2c* shows also that in addition to these remaining 'sharp' reflections, a broader reflection can be detected at a new position. *Figure 4* gives the microdensitometer readings from *cis*-$(CH)_x$ and *cis*-$(CH)_x$ slowly doped to a composition of $(CHI_{0.099})_x$. Three additional broad reflections are shown by arrows. *Table 1* gives spacings corresponding to these two series of Bragg reflections, in the *cis*-sample slowly doped to $(CHI_{0.099})_x$ and *cis*-$(CH)_x$ slowly doped to $(CHI_{0.14})_x$. In $(CHI_{0.099})_x$ only 6 sharp reflections and only 3 sharp reflections in $(CHI_{0.14})_x$ have been detected, with the three strongest reflections at spacing different from that in the undoped sample: 0.365 (0.368) nm, 0.212 (0.213) nm) and 0.183 (0.182) nm. These three spacings account very well with the reported lattice periodicities of *trans*-$(CH)_x$[7,11,16], particularly those by Fincher *et al.*[16] and Shimamura *et al.*[11] [(200)–(110), (020)–(310), (400)–(220) reflections, respectively, taking the *c*-axis in the chain direction]. A similar shift of the sharp reflections were observed for *cis*-$(CH)_x$ samples rapidly doped to a concentration $(CHI_{0.02})_x$ and higher (*Figure 2*).

The new broad reflections in the slowly-doped samples correspond to spacing at 0.79, 0.41 and 0.29 nm. The first spacing was the only one that had been previously reported by Hsu *et al.*[6]. This reflection was not observed in samples rapidly doped to much less than five per cent iodine. For the $(CHI_{0.099})_x$ sample, a Scherrer analysis of the linewidth gives a coherence length of 2.0 ± 0.5 nm for the three new broad reflections and a coherence length of $\approx$80 nm for the stronger, sharper reflections. This latter value is similar to the coherence length found in undoped $(CH)_x$.

Trans-$(CH)_x$ *samples*

The X-ray Debye–Scherrer pattern for *trans*-$(CH)_x$ is shown in *Figure 3a*. Comparison with *Figure 2a* shows that it differs from that of *cis*-$(CH)_x$ both in the position of Debye–Scherrer rings and in their relative intensity. The Debye–Scherrer pattern obtained from *trans*-$(CH)_x$ resembles in intensity and position that recently reported by

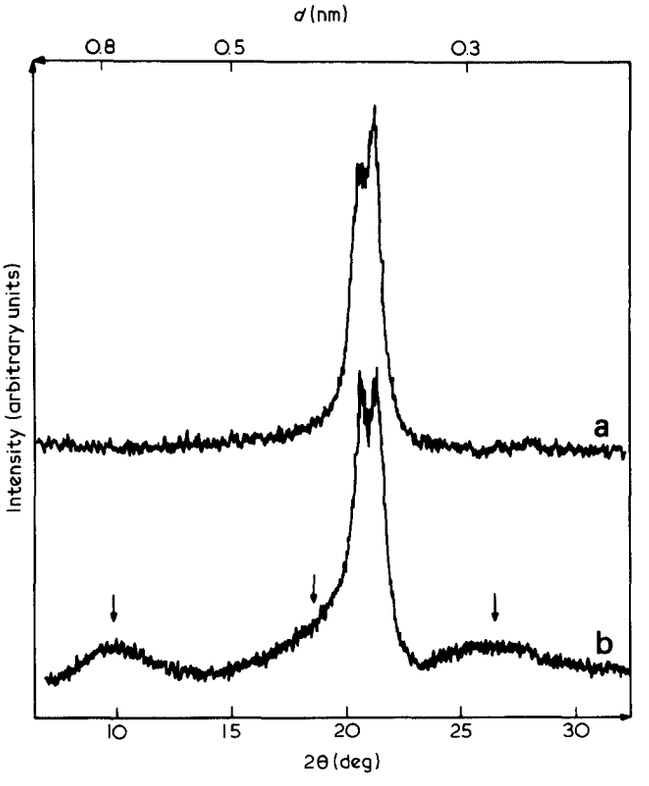

Figure 5 Microdensitometer readings from X-ray patterns (a) *trans*-$(CH)_x$ and (b) slow-doped *trans*-$(CHI_{0.05})_x$. Three additional broad reflections are shown by arrows. (λ=0.1315 nm)

Haberkorn *et al.*[17]. Spacings calculated from patterns obtained with CuKα and synchrotron radiations are given in *Table 2* and shows that the strongest reflection is in fact a doublet at 0.372 nm and 0.356 nm, which is further illustrated by the microdensitometer scan of *Figure 5a*. This splitting has been observed by Ito *et al.*[3] or by Haberkorn *et al.*[17], nor is there a report of such a splitting in the work of Shimamura *et al.*[11] and Fincher *et al.*[16]. Robin *et al.*[20] have recently shown that the doublet at 0.372 nm and 0.356 nm in *trans*-$(CH)_x$ correspond in fact to the splitting of the strongest 0.381 nm reflection of *cis*-$(CH)_x$ under isomerization. Taking into account this quoted doublet, the spacings of *trans*-$(CH)_x$ given in *Table 2* are in good agreement with those calculated using lattice periodicities by Baughman *et al.*[7] ($a_1 = 0.741$, $b_1 = 0.408$, $c_1 = 0.246$ nm). However, the doublet at 0.372 and 0.356 nm cannot be explained using the lattice periodicities of Fincher *et al.*[16] and Shimamura *et al.*[11], ($a_2 = 0.732$, $b_2 = 0.424$, $c_2 = 0.246$ nm). These and other spacings are also inconsistent with the two structures proposed by Lieser *et al.*[10]. While this requires a modified unit cell in the *a* and *b* directions, (the reflections are indexed as *hkO*), it does not necessarily refute the conclusion given by Fincher *et al.*[16] that there is an alternation of bond lengths parallel to the polymer chain.

As in the case of *cis*-$(CH)_x$, X-ray crystallinity of the *trans*-film was estimated at $\approx 90\%$ and the width of intense reflection gives a transverse coherence length of 8.0 ± 1.0 nm. Hence, neither the degree of crystallinity nor the crystallite size are significantly reduced by the isomerization process[20].

Iodine-doped trans-$(CH)_x$ *sample*

Figure 3 shows that iodine doping affects the X-ray patterns of *trans*-$(CH)_x$ and *cis*-$(CH)_x$ in a similar way. At low levels of doping there is no significant modification of the X-ray Debye–Scherrer pattern of the undoped compound. For more than five per cent iodine, reflections of pure *trans*-$(CH)_x$ strongly decrease in intensity and the weaker reflections of the undoped sample are no longer observed. As in heavily doped *cis*-$(CH)_x$, three new broad reflections have appeared. They are shown more clearly in the microdensitometer scan presented in *Figure 5b* for slowly-doped *trans*-$(CHI_{0.050})_x$. Spacings observed in slowly-doped *trans*-$(CHI_{0.125})_x$ are given in *Table 2*. In this case, the sharp reflections occur at the same positions as in the undoped sample. Only medium and strong reflections of undoped *trans*-$(CH)_x$ are observed in heavily-doped samples. The splitting at 0.372 and 0.356 nm is still visible. Neglecting this splitting, it is noteworthy that the three remaining sharp reflections of *cis*-$(CHI_{0.143})_x$ (*Table 1*) have the same spacings as the 3 remaining sharp reflections of *trans*-$(CHI_{0.125})_x$ (*Table 2*). *Table 2* shows also that, within experimental errors, broad reflections occur at the same positions as in heavily-doped *cis*-$(CH)_x$.

In the *trans*-$(CHI_{0.050})_x$ and *trans*-$(CHI_{0.125})_x$ samples, sharp reflections correspond to a coherence length of ≈ 8.0 nm and broad reflections to a coherence length of 2.0 ± 0.5 nm, similar to *cis*-$(CHI_{0.099})_x$. The slowly-doped *trans*-$(CHI_{0.125})_x$ sample was obtained from a similar starting piece of film as the undoped *trans*-$(CH)_x$; thus, it was possible to compare the relative intensity of the sharp diffraction lines (undoped regions) before and after doping. The results show that the crystalline region in pure *trans* has a volume fraction which is approximately double that of the undoped *trans* regions of $(CHI_{0.125})_x$. This implies that one half the volume of the $(CHI_{0.125})_x$ was undoped. Hence, the microscopic concentration of iodine in the doped areas is, on average, $(CHI_{0.25})_x$. Although high, this is less than the limiting composition obtained by packing considerations[6].

Comparison with other doped *trans* samples cannot be carried out because of the use of different radiation sources. Similarly, a comparison for *cis*-$(CH)_x$ is made more difficult because of the uncertainties in intensity normalization introduced by the observed shift with doping of the undoped sample reflections.

DISCUSSION

It has been shown[20] that thermal isomerization for *cis*-$(CH)_x$ to *trans*-$(CH)_x$ is not accompanied by a loss of crystallinity nor by a reduction of the transverse coherence length of crystals. Thus, the thermal isomerization process is homogenous within each crystal as the crystal must accommodate the increase of carbon periodicity in chain direction: the length of a *trans* unit (0.246 nm) being longer than the one of a *cis* unit (0.224 nm).

For more than five per cent iodine, two series of Debye–Scherrer rings are clearly observed. Sharp reflections keep the transverse coherence length (≈ 8.0 nm) and the position they have in undoped or slightly-doped *trans* samples, though they shift for *cis*-$(CH)_x$ and this indicates that they originate from undoped or weakly doped regions of $(CH)_x$ film. Broad reflections are observed only in heavily-doped samples and correspond to a coherence length of ≈ 2.0 nm. They can be associated with heavily-doped regions of the polyacethylene film. Observation of these two series of reflections proves that the films are inhomogeneously doped. Energy dispersive X-ray analysis[26] of iodine concentration through the thickness of the film and along the surface of the film demonstrate that the iodine concentration in highly-doped samples in uniform to within a resolution of 500 nm. This suggests that the doped regions are in the outer volume of individual fibrils[25]. In *cis*, iodine-doped samples, lateral spacings corresponding to the undoped regions (sharp reflections of *Table 1*) are very close to those observed in a *trans* crystalline structure. This suggests that iodine induces an isomerization of the undoped regions of the *cis* sample. This dopant-induced isomerization of the undoped regions may be due to removal of an electron from the pi-orbital of the *cis* sample allowing easier bond rotation. Alternatively, the crystals which make up the outer layer of fibrils should elongate parallel to the fibre direction upon doping. This stress induces a strain parallel to the chain axis in undoped inner crystals (polymer chain being parallel to the fibre axis[13]). As *trans*-$(CH)_x$ chains are $\approx 10\%$ longer than *cis*-$(CH)_x$ chains, this strain may induce isomerization. Such an effect has been observed for mechanical rolling of *cis*-$(CH)_x$ films[36,37].

The sharp reflections decrease in intensity with the increasing amount of dopant suggesting that for high concentrations, iodine enters into the crystalline part of fibrils where it breaks the lateral periodicities between polyacetylene chains and swells the fibrils[26]. The observation of broad reflections shows that for a limited coherence length, iodine and polyacetylene undergo some ordering. On the basis of the observation of the first reflection at 0.78 nm, Bauchman *et al.*[5] have suggested

that iodine species intercalate in sheets between closely packed adjacent planes of polyacetylene chains (planes (100) using the choice of axis of ref. 5). Here, there is evidence of two additional reflections at 0.41 and 0.29 nm, confirming this ordering, both in heavily-doped *cis*-$(CH)_x$ and *trans*-$(CH)_x$. Furthermore, in recent published data[13] for *trans*- and *cis*-polyacetylene doped with AsF_5, three similar reflections at 0.84, 0.41 and 0.31 nm are evident.

Spectroscopic measurements[6] show that iodine is present in $(CH)_x$ mostly in the form of I_3^- units. As the length of an I_3^- unit (0.96[38]–1.01[39] nm) is not a simple multiple of the periodicity of *cis* units along the chains[5], an ordering between these entities in the chain direction seems to be more difficult than in the transverse direction. The I_3^- length is, however, approximately equal in length to four repeat distances along the chain of *trans*-$(CH)_x$[16] ($4 \times 0.246 = 0.984$ nm). Similar results concerning AsF_5-doped $(CH)_x$ support the association of the periodicity related to these broad reflections with lateral ordering between iodine and polyacetylene. In an intercalation model[5], the spacing corresponding to the first reflection observed is equal to the sum of the diameter of a $(CH)_x$ chain and that of an I_3-unit. As there are two $(CH)_x$ close-packed planes per unit cell, between which iodine intercalates, the new lattice periodicity is equal to twice the spacing of the first reflection.

Here, this periodicity along the (100) direction leading to $a_I = 1.59$ and $a_{AsF_5} = 1.68$ nm, is used. The other transverse direction, situated in the close-packed plane of $(CH)_x$ is not changed by the intercalation. Using the parameter b_2 determined for *trans*-$(CH)_x$ ($b_I = b_{AsF_5} = 0.424$ nm)[11,16], *Table 3* gives the lateral spacing found with this unit cell for both iodine- and AsF_5-doped $(CH)_x$. Several spacings are close to the experimentally determined values of 0.41 and (0.29–0.31) nm. A small decrease of some of the lateral spacings is obtained if the parameter $b_1 = 0.408$ nm is used[7] instead of b_2. This effect, smaller than the experimental errors in the determination of spacings, does not change the results of this analysis. The long a spacing used includes two layers of $(CH)_x$ chains of opposite setting angle. The dopant is assumed to intercalate between each layer of $(CH)_x$, i.e., there are two layers of dopant within the new unit cell. It is noted that if the periodicity a is divided by two, (i.e., there is only one $(CH)_x$ plane and one iodine plane as the repeat unit in the a direction) then only those reflections in *Table 3* with event h are allowed. The three new reflections observed with I_2 doping as well as the three new reflections reported[13] for AsF_5-doped $(CH)_x$, can be accounted for by this new unit cell.

Table 3 Transverse spacing calculated using units cell (a_I = 1.58, b_I = 0.424 nm) and (a_{AsF_5} = 1.68, b_{AsF_5} = 0.424 nm). Dividing the periodicity along a by two suppresses all reflections with an odd index h. AsF_5-doped $(CH)_x$ data is from ref. 13

Reflections (*hkl*)	Calculated spacing, I_2-doped $(CH)_x$ (nm)	Observed spacing, I_2-doped $(CH)_x$ (nm)	Calculated spacing, AsF_5-doped $(CH)_x$ (nm)	Observed spacing, AsF_5-doped $(CH)_x$ (nm)
100	1.58		16.8	
200	0.79	0.79	0.84	0.84
300	0.53		0.56	
010	0.424		0.424	
110	0.41	0.41	0.41	0.41
400	0.395		0.42	
210	0.37		0.38	
310	0.33		0.34	
500	0.315		0.336	
410	0.29	0.29	0.30	0.31

CONCLUSIONS

An extensive X-ray and synchrotron radiation diffraction study has been carried out of the evolution of the structures of *cis*-$(CH)_x$ and *trans*-$(CH)_x$ upon doping with iodine. Studies of iodine-doped *cis*- and *trans*-$(CH)_x$ confirmed that even at the highest doping level studied ($(CHI_{0.2})_x$, an undoped region of $(CH)_x$) remains. Two new, previously unreported X-ray lines associated with iodine-doped $(CH)_x$ were recorded for both *cis*- and *trans*-doped materials. The X-ray structures for iodine-doped *cis*- and iodine-doped *trans*-$(CH)_x$ are almost identical, independent of dopant concentration with transverse coherence lengths of ≈ 2.0 nm. These results are consistent with the model of intercalation of iodine between planes of close packed *trans*-polyacetylene chains.

ACKNOWLEDGEMENTS

The authors are very grateful to S. Megtert for his assistance on the station D 16 of LURE.

REFERENCES

1 Chiang, C. K., Fincher, C. R., Jr., Park, Y. W., Heeger, A. J., Shirakawa, H., Louis, E. J., Gau, S. C. and Mac Diarmid, A. G. *Phys. Rev. Lett.* 1977, **39**, 1098
2 For recent reviews see: Proceedings of the International Conference on Low-Dimensional Conductors, Boulder Colorado, August 9–14, 1981, (Eds. A. J. Epstein and E. M. Conwell (Molecular Crystals Liquid Crystals 1981, **77** and 1982, **83**); and Proc. Int. Conf. on the Physics and Chemistry of Conducting Polymer, Les Arcs, Savoie, France. 11–15 Décembre (1982) (Ed. R. Comes) *J. de Physique* in press
3 Ito, T., Shirakawa, H. and Ikeda, S. *J. Polym. Sci., Polym. Chem. Edn.* 1974, **12**, 11; 1975, **13**, 11
4 Karpfen, A. and Holler, R. *Solid State Commun.* 1981, **37**, 179
5 Baughman, R. H., Hsu, S. L., Pez, G. P. and Signorelli, A. J. *J. Chem. Phys.* 1978, **68**, 5405
6 Hsu, S. L., Signorelli, A. J., Pez, G. P. and Baughman, R. H. *J. Chem. Phys.* 1978, **69**, 106
7 Baughman, R. H., Hsu, S. L., Anderson, L. R., Pez, G. P. and Signorelli, A. J. *Nato Conf. Ser.* 1979, Series **6**, 187
8 Asaishi, T., Miyasaka, K., Ishikawa, K., Shirakawa, H., Ikeda, S. *J. Polym. Sci., Polym. Phys. Edn.* 1980, **18**, 745
9 Lieser, G., Wegner, G., Muller, W. and Enkelmann, V. *Makromol. Chem., Rapid Commun.* 1980, **1**, 621
10 Lieser, G., Wegner, G., Muller, W., Enkelmann, V. and Meyer, W. H. *Makromol. Chem., Rapid Commun.* 1980, **1**, 627
11 Shimamura, K., Karasz, F. E., Hirsch, J. A. and Chien, J. C. W. *Makromol. Chem., Rapid Commun* 1980, **2**, 473
12 Enkelmann, V., Lieser, G., Muller, W. and Wegner, G. *Chemica Scripta* 1981, **17**, 141
13 Stamm, M., Hocker, J. and Axmann, A. *Mol. Cryst. Liq. Cryst.* 1981, **77**, 125
14 Enkelmann, V., Lieser, G., Monkenbusch, M., Muller, W. and Wegner, G. *Mol. Cryst. Liq. Cryst.* 1981, **77**, 111
15 Monkenbusch, M., Morra, B. S. and Wegner, G. *Makromol. Chem., Rapid Commun.* 1982, **3**, 69
16 Fincher, C. R., Jr., Chen, C. E., Heeger, A. J., Mac Diarmid, A. G. and Hastings, J. B. *Phys. Rev. Lett.* 1982, **48**, 100
17 Haberkorn, H., Naarmann, H., Penzien, K., Schlag, J. and Simak, P. *Synthetic Metals* 1982, **5**, 51
18 Chien, J. C. W., Karasz, F. E. and Shimamura, K. *Macromolecules* 1982, **15**, 1012

19 Deits, W., Cukor, P., Rubnor, M. and Jopson, H. *J. Electr. Mat.* 1981, **10**, 683

20 Robin, P., Pouget, J. P., Comes, R., Gibson, H. W. and Epstein, A. J. *Phys. Rev. B* 1983, **27**, 3938

21 Clarke, T. C., McQuillan, B. W., Rupolt, J. F., Scott, J. C. and Street, G. B. *Mol. Cryst. Liq. Cryst.* 1982, **83**, 1; Clarke, T. C. and Scott, J. C. *Solid State Commun.* 1982, **41**, 389

22 Kuzmany, H. *Phys. Stat. Sol.* (*b*) 1980, **97**, 521

23 Hoffman, D. M., Tanner, D. B., Epstein, A. J. and Gibson, G. W. *Phys. Rev. B* 1983, **27**, 1454

24 Feldblum, A., Kaufman, J. H., Etemad, S., Heeger, A. J., Chung, T. C. and Mac Diarmid, A. G. *J. Chem. Phys.* 1982, **77**, 5114

25 Epstein, A. J., Rommelmann, H., Druy, M. A., Heeger, A. J. and Mc Diarmid, A. J. *Solid State Commun.* 1981, **38**, 683

26 Epstein, A. J., Rommelmann, H., Fernquist, R. Gibson, H. W., Druy, M. A. and Woerner, T. *Polymer* 1982, **23**, 1211

27 Epstein, A. J., Gibson, H. W., Chaikin, P. M., Clark, W. G. and Gruner, G. *Phys. Rev. Lett.* 1980, **45**, 1730

28 Epstein, A. J., Rommelmann, H., Abkowitz, M. and Gibson, H. W. *Phys. Rev. Lett.* 1981, **47**, 1549

29 Hoffmann, D. M., Tanner, D. B., Epstein, A. J. and Gibson, H. W. *Mol. Cryst. Liq. Cryst.* 1982, **83**, 1175

30 Epstein, A. J., Rommelmann, H., Bigelow, R., Gibson, H. W., Hoffmann, D. M. and Tanner, D. B. *J. de Physique* in press

31 Epstein, A. J., Rommelmann, H., Bigelow, R., Gibson, H. W., Hoffmann, D. M., Tanner, D. B., Robin, P., Comes, R. and Pouget, J. P. to be published

32 Mott, N. F. and Davis, E. A. 'Electronic Processes in Non-Crystalline Materials', Clarendon, Oxford, 1979

33 Rice, M. J. *Phys. Lett.* 1979, **71A**, 152; Su, W. P., Schrieffer, J. R. and Heeger, A. J. *Phys. Rev. Lett.* 1979, **42**, 1698

34 Mele, E. J. and Rice, M. J. *Phys. Rev. B* 1981, **23**, 5397

35 Guinier, A. 'Theorie et Technique de la Radiocristallographie' Dunod, 1956

36 Vansco, G., Egyed, O., Pekker, S. and Janossy, A. *Polymer* 1982, **23**

37 Robin, P. unpublished result

38 Coppens, P., Leung, P., Murphy, K. E., Tilborg, P. R. V., Epstein, A. J. and Miller, J. S. *Mol. Crystal. Liq. Cryst.* 1980, **61**, 1

39 Miller, J. S. and Griffiths, C. H. *J. Am. Chem. Soc.* 1977, **99**, 749